

# Elastin-like recombinamers with acquired functionalities for gene-delivery applications

AQ3

Maria J. Piña,<sup>1</sup> Susan M. Alex,<sup>2</sup> Francisco J. Arias,<sup>1</sup> Mercedes Santos,<sup>1</sup> Jose C. Rodriguez-Cabello,<sup>1</sup> Rehka R. Mannemcherril,<sup>2</sup> Chandra P. Sharma<sup>2</sup>

<sup>1</sup>Bioforge Research Group, University of Valladolid, CIBER-BBN, Valladolid 47011, Spain

<sup>2</sup>Biosurface Technology, Biomedical Technology Wing, Sree Chitra Tirunal Institute for Medical Sciences and Technology, Poojappura, Thiruvananthapuram, Kerala 695 012, India

Received 18 December 2014; revised 26 February 2015; accepted 10 March 2015

Published online 00 Month 2015 in Wiley Online Library ([wileyonlinelibrary.com](http://wileyonlinelibrary.com)). DOI: 10.1002/jbm.a.35455

**Abstract:** In this work, well-defined elastin-like recombinamers (ELRs) were studied as a choice to the existing nonviral vectors due to their biocompatibility and ease of scale-up. Functional motifs, namely penetratin and LAEL fusogenic peptides were incorporated into a basic ELR sequence, and imidazole groups were subsequently covalently bound obtaining ELRs with new functionalities. Stable polyplexes composed of plasmid DNA and ELRs were formed. A particle size around 200 nm and a zeta potential up to nearly +24 mV made them suitable for gene delivery purposes. Additionally, viability and transfection

assays with C6 rat glioma cell line showed an increase in the cellular uptake and transfection levels for the construction containing the LAEL motif. This study highlights the importance of controlling the polymer functionality using recombinant techniques and establishes the utility of ELRs as biocompatible nonviral systems for gene-therapy applications. © 2015 Wiley Periodicals, Inc. *J Biomed Mater Res Part A*: 00A:000–000, 2015.

**Key Words:** ELR, elastin-like recombinamers, gene therapy, cationic polymers, polyplex

**How to cite this article:** Piña MJ, Alex SM, Arias FJ, Santos M, Rodriguez-Cabello JC, Mannemcherril RR, Sharma CP. 2015. Elastin-like recombinamers with acquired functionalities for gene-delivery applications. *J Biomed Mater Res Part A* 2015;00A:000–000.

## INTRODUCTION

The importance of gene therapy is directly reflected by the increasing number of clinical trials conducted over the past few years.<sup>1</sup> A large number of diseases, including some cancers, monogenetic disorders, and cardiovascular, neurological and immune diseases, amongst others, are increasingly being seen as possible targets for gene-therapy studies.<sup>2–4</sup> The success of gene-therapy treatment depends on both the genetic material concerned and on the carrier. Naked DNA molecules cannot pass through the cell membrane due to its negative charge; in addition, they are rapidly degraded because of their high susceptibility to nucleases.<sup>5</sup> As such, vectors are a critical element in the gene-delivery process. The most important attributes for the “ideal” delivery vector are biocompatibility and an ability to release the cargo into a specific target. In this regard, a great deal of research effort has been focused on viral vectors, especially retro- and adenoviruses. However, the inflammatory response in the receptor organism and complications when scaling up

production make nonviral vectors an excellent alternative.<sup>6–9</sup> Although nonviral vectors, such as cationic polymers, exhibit lower transfection efficiency than viral vectors, they present some advantages, namely that they generally have low host immunogenicity, which would allow repeated administration, and are easier to produce on a large scale.<sup>10</sup> Cationic polymers are preferred due to their ability to condense DNA by electrostatic interactions with the negatively charged phosphates from the genetic material. This results in a tight DNA-polymer complex, also known as a polyplex, which protects the contents from degradation by the enzyme nuclease.<sup>11</sup>

The extra- and intracellular obstacles that DNA-polymer complexes encounter on their way to the target must be taken into account when designing a gene-delivery system. Firstly, anatomical barriers and subsequently the plasma membrane are some of the most limiting steps in transfection. Molecules with a positive surface charge, such as cationic polymers, tend to interact better with the plasma

Additional Supporting Information may be found in the online version of this article.

**Correspondence to:** J.C. Rodríguez-Cabello (e-mail: [roca@bioforge.uva.es](mailto:roca@bioforge.uva.es))

Contract grant sponsor: ERDF Funding from the EU and MINECO; contract grant number: MAT2010-15982

Contract grant sponsor: FCCI Subprogram: Modality ACI-COLABORA Spain-India 2010-2012; contract grant numbers: MAT2010-15310, PRI-PIBAR-2011-1403, MAT2012-38043, and MAT2013-41723-R

Contract grant sponsor: JCyL; contract grant numbers: VA049A11, VA152A12, and VA155A12

Contract grant sponsor: CIBER-BBN, JCyL, and the Instituto de Salud Carlos III under the “Network Center of Regenerative Medicine and Cellular Therapy of Castilla and Leon” and DST (Indo-Spanish), (New Delhi)

membrane.<sup>12</sup> In addition to the surface charge of the macromolecule, size is another parameter that must be kept in mind. Particles with a size smaller than 1  $\mu\text{m}$  tend to be internalized by phagocytosis and those of around 200 nm by endocytic processes.<sup>13</sup> Furthermore, rather than the surface charge, other systems, such as certain arginine-rich peptides, exhibit high efficacy in the internalization process.<sup>14,15</sup> Molecules that enter via the endocytosis pathway experience a drop in pH from physiological to pH 6, with subsequent further reduction to pH 5 during progression from late endosomes to lysosomes and the presence of lytic enzymes. Some escape mechanisms have been studied to release complexes from the endosome. One such approach involves the use of fusogenic molecules in order to disrupt the endosome membrane,<sup>16</sup> whereas another involves the use of weak amine groups such as imidazole with an effect similar to the cationic polymer PEI (polyethyleneimine). PEI acts on the osmotic pressure within the endosome, causing the vesicle to rupture as a result of the called "proton sponge effect." When the complexes formed by these compounds and nucleic acids are internalized into the cell, they are able to buffer the endosomal vesicle, leading to endosomal swelling and lysis, thus releasing the nucleic acids into the cytoplasm.<sup>10,17,18</sup> However, the main problem of PEI is its cytotoxicity, causing cell apoptosis in a wide number of human cell lines.<sup>19</sup> The cytocompatibility nature of the material forming the polyplexes and their ability to overcome these natural barriers will therefore determine the success of the system.<sup>20,21</sup>

Elastin-like recombinamers (ELRs) are polymers with increasing applications in different fields, such as tissue engineering, protein purification, cell harvesting, and smart and bioactive surfaces.<sup>22–24</sup> These compounds are based on the hydrophobic domain of natural elastin, which is one of the main components of the extracellular matrix. They are composed of repetitions of the pentapeptide (Val-Pro-Gly-X-Gly), or its permutations, where X is a guest residue that can be any amino acid except proline. The smart nature of ELRs resides in their characteristic transition temperature ( $T_t$ ). Below this temperature, the ELR chains are hydrophobically hydrated, forming a disordered state of random coils, whereas above  $T_t$  the structure loses its water molecules to form a phase-separated state in which the ELRs adopt a dynamic, regular, and ordered  $\beta$ -spiral structure,<sup>25</sup> thereby resulting in a variation in enthalpy. This folding is reversible if the temperature is decreased below  $T_t$ .<sup>25</sup> The similarity with native elastin endows ELRs with biocompatibility, smart behavior, and excellent mechanical properties. The biocompatibility of such compounds has been tested by the ASTM (American Section of the International Association for Testing Materials) and confirmed in numerous other studies.<sup>26</sup> Recent studies have suggested that ELRs are promising materials for delivery purposes<sup>27</sup> by demonstrating the use of ELRs fused to a cell penetrating peptide (CPP) as a drug delivery vector for solid tumors.<sup>16,17,28</sup> Additionally, a similar combination of ELRs fused to CPPs has been utilized to deliver therapeutic peptides into target tumor cells.<sup>29</sup>

We hypothesized that, given the properties of ELRs, the lysine-based vector with the sequence  $((\text{VPGIG})_2(\text{VPGKG})(\text{VPGIG})_2) \times 24$  modified with different functional motifs namely penetratin, the fusogenic peptide LAEL and imidazole addition is able to improve the delivery of genetic material inside the cells tested in *in vitro* assays with low cytotoxicity.

## MATERIALS AND METHODS

### ELR biosynthesis and characterization

Standard molecular-biology techniques were used to create the polymers IK120, IK120CPP, and LAELIK120CPP.<sup>23</sup> ELRs were based on the Val-Pro-Gly-Xaa-Gly (VPGXG) structure, where X is isoleucine or lysine:  $((\text{VPGIG})_2(\text{VPGKG})(\text{VPGIG})_2) \times 24$  and containing the bioactive CPP (RQI-KIWFQNRMRMKWKK) and LAELLAELLAEL domains. Addition of the monomeric genes was accomplished in a stepwise manner using the recursive directional ligation method, and polymers with a specific length and molecular weight were produced as described elsewhere.<sup>30</sup>

A chemical amidation reaction was applied during the synthesis of IMID-IK120 in order to incorporate imidazole groups into the IK120 lysine-enriched amino acid sequence.

The ELR sequences were transformed into *Escherichia coli* BLR (DE3) strain (Stratagene, La Jolla, CA) for production. The purification process involved cycles of temperature-dependent and reversible precipitation.<sup>31</sup> Endotoxins were removed using an additional NaCl and NaOH treatment.<sup>32</sup>

All polymers were characterized by sodium dodecyl sulfate-polyacrylamide gel electrophoresis (SDS-PAGE), mass spectrometry (MALDI-TOF), proton nuclear magnetic resonance analysis (H-NMR), differential scanning calorimetry (DSC), and amino acid analysis. Endotoxin levels were measured using the Endosafe-PTSTM test (Charles River, Wilmington, MA).

### Synthesis of IMID-ik120

Imidazole functional groups were conjugated to the lysine amino acids in IK120 as follows.

A solution of NHS (12 equiv.) in MES (2-(*N*-morpholino)ethanesulfonic acid buffer) was added to a solution of EDAC (1-ethyl-3-(dimethylaminopropyl) (Sigma Aldrich, St. Louis, MO) (12 equiv.) in MES at pH 4.5. EDAC acts as an activating agent for the carboxyl group. The resulting mixture was stirred at 4 °C for 1 h and a solution of 1-*H*-imidazole-2-carboxylic acid (10 equiv.) in MES buffer was then added. This mixture was stirred at 4 °C for 1 h. After this time, a freshly prepared solution of IK120 ELR (1 equiv.) in MES was added and the reaction mixture stirred at 25 °C for 72 h. The IMID-IK120 obtained was diluted in deionized water, dialyzed and lyophilized. Incorporation of the imidazole groups was corroborated by DSC and H-NMR.

### Thermal behavior

All the ELR polymers were dissolved in PBS 1 $\times$  (Sigma Aldrich, St. Louis, MO) at 50 mg/mL at 4 °C 24 h before of the measurement. Thermal behavior was accomplished by DSC using a Mettler Toledo 822e with liquid-nitrogen cooler.

The heating program included an initial isothermal stage (5 min at 0 °C), followed by heating at 5 °C/min from 0 °C to the desired temperature of around 55 °C.

To assess the incorporation of the imidazole groups in IMID-IK120, the polymer was dissolved at 50 mg/mL in deionized water for 24 h at 4 °C and adjusted to pH 10.7, 8.0, and 3.5 with NaOH 1M and HCl 1M. Consecutive measurements were accomplished at pH 10.7, 8.0, and 3.5 with the previously described method.

### Buffering capacity

The buffering capacities of ELRs were measured as follows. A 2.5 mg sample of the ELR was dissolved in 25 mL of 0.9% NaCl to a final concentration of 0.1 mg/mL and stored at 4 °C overnight. The initial pH of the polymer solution was adjusted to 10 with 0.2N NaOH and titrated by gradual addition of 50 µL aliquots of 0.01N HCl. The pH values for all solutions were measured using a pH-meter (Crison GLP22). PEI 25 kDa (Sigma Aldrich, St. Louis, MO) was used as control.

### Hemocompatibility studies

Hemocompatibility studies were performed with blood from non-medicated healthy human donors and collected in tubes containing 3.8% sodium citrate at a 9:1 (blood:anticoagulant) ratio. IK120, IMID-IK120, IK120CPP, and LAE-LIK120CPP were dissolved in 0.9% NaCl at a concentration of 1 mg/mL. For each assay, 100 µg of ELR was required.

**Red blood cell (RBC) aggregation.** After centrifugation of the anticoagulated blood at 700 rpm for 10 min, the plasma and red blood cell fraction were separated. The RBC fraction was diluted in 0.1M PBS pH 7.4 (8:1); 100 µL of red blood cells was incubated for 30 min with 100 µL of ELR solution or PEI (1 mg/mL). PEI 25 kDa was used as positive control and 0.9% NaCl as negative control.

**White blood cell (WBC) and platelet blood cell (PBC) aggregation.** For separation of WBC and platelets, blood was layered over an equal amount of Histopaque 1077 (Sigma Aldrich, St. Louis, MO) in clean glass tubes. Centrifugation was carried out at 800 rpm for 15 min to obtain the upper yellow (platelet blood cells) and middle white blood cells. White blood and platelet cells were incubated with 100 µg of ELR or PEI for 30 min.

The aggregation results were observed under a Leica DF295 microscope.

### Cell culture

*In vitro* and transfection experiments were performed using the C6 glioma cell line from rat (ATCC® CCL-107, ATCC, Middlesex, UK). C6 cells were chosen as it has been widely used as suitable gene therapy host in glioblastoma research.<sup>33-35</sup> Cells were seeded in culture flasks with DMEM medium in 10% FBS and incubated at 37 °C for 24 h in 5% CO<sub>2</sub> with 95% humidity to obtain a growth confluence of 80%. Cells were then trypsinized and transferred to multiwell tissue culture plates.

### *In vitro* viability assay of ELRs

The cell viability of IK120-based ELRs was evaluated using the Alamar Blue and Live/Dead assays (Life Technologies, Carlsbad, CA) on C6 cells. Cells were seeded on 96-well plates at 5000 cells/cm<sup>2</sup> in 100 µL DMEM medium with 10% FBS for 24 h. After that time, the medium was discarded and cells were incubated for 24 h with 5 µL ELR dissolved at different concentrations and made up to 100 µL with FBS-free medium. For the Alamar Blue assay, the polymers were removed after 24 h and 100 µL Alamar Blue solution was added to each well to a final concentration of 1%. PEI at 20 µg/mL was used as reference polymer. Untreated cells were considered to calculate the % cell viability. The fluorescence intensity (F.I.) of test samples and controls was measured at an emission wavelength of 590 nm after excitation at 560 nm using a SpectraMax M2 microplate reader (Molecular Devices, Sunnyvale, CA). Cell viability was calculated as:

$$\% \text{ Cell viability} = 100 \times \left( \frac{\text{F.I. Treated cells}}{\text{F.I. Untreated cells}} \right)$$

For the Live/Dead assay, after removing the polymers, 50 µL each of a solution of calcein AM and ethidium homodimer-1 were added to each well at a final concentration of 2 µM and 4 µM in D-PBS, respectively. The plate was then incubated in the dark at room temperature for 30 min and visualized under a fluorescence microscope (Nikon eclipse Ti-SR, Japan).

### Preparation of ELR complexes

Cationic ELR-based polymers underwent rapid complex formation with the negatively charged plasmid DNA. Thus, the ELR was dissolved to a concentration of 1 mg/mL in deionized water at 4 °C overnight. Plasmid DNA was also prepared with the same concentration of 1 mg/mL. Nanoparticles were formed in aqueous solution by mixing the pDNA with the ELR solution at the appropriate weight ratio. The mixtures were vortexed at 10 °C for 1 min and incubated at 4 °C for 20 min for nanocomplex formation. After this incubation the temperature was increased to 37 °C for immediate application.

### Gel retardation assay

The ELR-pDNA complexes at different pDNA/ELR weight ratios (10/1, 40/1, 80/1, 120/1, and 140/1) were loaded onto a 1% agarose gel. Electrophoresis was carried out in 1× TBE buffer (89 mM Tris-HCl pH 8.3, 89 mM borate, and 2 mM EDTA), staining with 2 µL of 10 mg/mL ethidium bromide. Electrophoresis was run at room temperature at 100 mV for 60 min in a Bio-Rad electrophoresis device (Bio-Rad laboratories, CA). The complexed pDNA was visualized and photographed using a MultiImage TM Light Cabinet (Alpha Innotech Corporation, San Leandro, CA).

### Stability assay

For the stability assay, nanocomplex formation at ELR/pDNA weight ratios of 10/1, 40/1, 80/1, 120/1, and 140/1

was performed. The resulting nanocomplexes were incubated with 20  $\mu$ L of plasma, from nonmedicated healthy human donors, for 30 min.<sup>36</sup> The displacement was detected by 1% agarose gel electrophoresis and visualized using a MultiImage TM Light Cabinet (Alpha Innotech Corporation, San Leandro, CA).

#### Determination of particle size and zeta potential

The particle size and zeta potential of the nanocomplexes were determined by Dynamic Light Scattering (DLS) using a Zetasizer Nano ZS (Malvern Instruments Ltd., UK) at a temperature of 15 °C for 40/1, 80/1, 120/1, and 140/1 ratios. Z-average mean (nm) and zeta potential (mV) were used for data analysis.

#### Transmission electron microscopy

TEM measurements were performed using a JEOL JEM-1230 electron microscope operating at 120 kV. The polyplex solution of ELR and pDNA was dropped onto carbon-coated copper grids and images recorded after drying for 5 min at room temperature.

#### Cell-transfection studies

**P53 expression.** C6 cells were seeded into four-well plates in a quantity of  $1 \times 10^4$  per well and allowed to grow at 37 °C under 5% CO<sub>2</sub> overnight.

ELRs and pCMV-p53 plasmid (Clontech, CA) were used to form nanocomplexes at two different ELR:pDNA weight ratios (80/1 and 120/1). The cells were incubated with the nanocomplexes at 37 °C under 5% CO<sub>2</sub> for 5 h. After this time, the medium was replaced with fresh medium and the cells incubated for a total of 48 h. Before the assay, the cells were washed twice with PBS. A 250  $\mu$ L aliquot of calcein AM ethidium homodimer-1 reagent solution was added and the mixture left in the dark at room temperature for 30 min. After this time, the reagent was discarded and 400  $\mu$ L PBS added. The state of the cells was visualized using a fluorescence microscope (Leica DMI 3000 B, Germany).

**Polyplex cell internalization.** A total of  $1 \times 10^4$  C6 cells per well were seeded onto four-well plates and allowed to grow overnight at 37 °C under 5% CO<sub>2</sub>. p53 plasmid was tagged with YOYO iodide by incubation for 1 h in the dark. ELR/pDNA nanocomplexes were prepared at a ratio of 80/1 and the cells incubated for 3 h with these complexes. Nuclear staining was performed using Hoechst by incubation at 37 °C under 5% CO<sub>2</sub> for 30 min. The cells were then washed with PBS and viewed under the fluorescence microscope.

**Luciferase expression.** A total of  $3.5 \times 10^4$  C6 cells per well were seeded onto 96-well plates and grown at 37 °C under 5% CO<sub>2</sub> overnight. After this time the cells were incubated with the polyplexes (80/1 weight ratio) formed with a plasmid containing the luciferase gene (pRNA-Luc/Neo, GenScript, Piscataway, NJ) in a serum-free medium for 5 h. The medium was then replaced by fresh serum-containing medium and the cells cultured for a further 48 h. At this

point the cells were lysed with 100  $\mu$ L Glo lysis buffer (Promega). The Bright Glo luciferase assay system (Promega) was added in a 1:1 proportion of lysate and luciferase reagent. The light produced was measured using a luminometer (SpectraMax L, Molecular Devices). The protein content of the lysate was determined by a Bradford assay using a microplate reader. Luciferase expression is given as relative light units (RLU) per  $\mu$ g of protein.

#### Statistical analysis

Inter-group comparisons were performed using Scheffe's test, with *p* values of less than 0.05 indicating statistical significance.

## RESULTS

### Synthesis and characterization of IK120CPP, LAELIK120CPP, and IMID-ik120

The ELRs were designed using an existing ELR cationic backbone in order to condense the plasmid DNA and interact with the negatively charged plasmatic membrane. Novel ELRs containing the bioactive domains CPP (RQI-KIWFQNRMRMKWKK) and LAEL (LAELLAELLAEL) were synthesized using genetic-engineering techniques. The bioactive domains were introduced by recursive directional ligation (RDL), which allows full control of the composition, chain length, architecture and physicochemical properties of the ELRs and therefore giving them an advantage with respect to other polymers<sup>30</sup> (Fig. 1). The yields for these polymers in *Escherichia coli* were 35 and 50 mg/L, respectively (Table I). The decrease in the yield for IKCPP was attributed to destabilization of the bacterial membrane by CPP. The polymer IMID-IK120 was constructed by chemical incorporation of imidazole 2-carboxylic acid into the IK120 cationic backbone (Supporting Information Fig. S1). Schematic constructs for all polymers studied can be found in Figure 1.

The final products were characterized by SDS-PAGE electrophoresis (data not shown), mass spectrometry (MALDI-TOF), nuclear magnetic resonance (H-RMN), differential scanning calorimetry (DSC), and amino acid analysis (Supporting Information Figs. S2–S5). The endotoxin levels were <50 EU/mg.

#### Thermal behavior of the ELRs

The smart nature of the polymers was studied by DSC with the polymers dissolved in PBS (Table II). They were found to behave as self-assembled systems with a transition temperature (*T<sub>t</sub>*) of around 30 °C, which would permit their use at an optimal temperature of 37 °C for gene-delivery applications. All the ELRs in this study varied their enthalpies, thus resulting in endothermic processes.

A deeper study of the thermal behavior for the IMID-IK120, was conducted (Fig. 2 and Supporting Information Table S1). As such, the *T<sub>t</sub>* increased as the polarity increased with decreasing pH. Indeed, at pH 10.7 basification of the medium is sufficiently high that the amino groups of the lysines (*pK<sub>a</sub>* 10.5) from the polymer are largely deprotonated. This reduces the mean polarity of the molecule, thereby producing a decrease in *T<sub>t</sub>* to 18.5 °C. Moreover, as

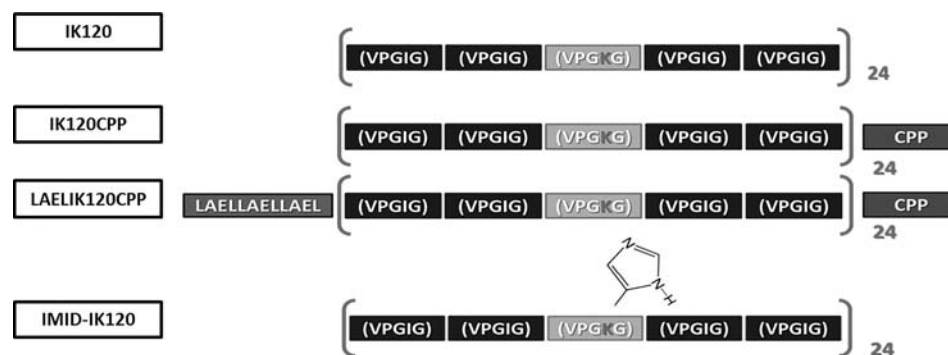


**FIGURE 1.** Schematic representation of the ELR constructs. [Color figure can be viewed in the online issue, which is available at [wileyonlinelibrary.com](http://wileyonlinelibrary.com).]

AQ4

the  $pK_a$  of the imidazole is around 6.9, this group is deprotonated above pH 7, thereby intensifying the reduction of  $T_t$ . However, the variation in  $T_t$  at a pH of between 10.7 and 8.0 (22.6 °C) indicated that not all the lysines had been modified with imidazole groups and that their amino groups had therefore been protonated. The NMR spectra showed signals at 7.7 ppm corresponding to H-N1 and H-C5 protons from imidazole. Moreover, the  $CH_2$  group vicinal to the amide groups appeared at 2.9 ppm. Integration of the peaks led to a substitution percentage of 65% (Supporting Information Fig. S4). Finally, a significant increase of 10 °C in  $T_t$  was observed at pH 3.5 (32.4 °C) as a result of protonation of the imidazole groups.

### Buffering capacity

To evaluate the protonation ability of ELRs in general and imidazole groups for IMID-IK120 in particular, both ELRs and PEI as reference polymer were titrated against 0.01N HCl from pH 10.0 to pH 4.0.

Our findings showed that PEI polymer possessed larger buffering effect than ELRs especially at physiological pH (7–5). However, at these concentrations, IMID-IK120 showed a milder increase in buffering capacity in the pH range 8 to 6 than the other ELRs, thereby correlating with protonation of the imidazole groups (Fig. 3).

F3

### Blood compatibility assays

Blood cell aggregation studies with the red blood cell fraction (Fig. 4), white cells and platelets (Supporting Information Figs. S6 and S7) were carried out. The results showed no aggregation with any of the blood cells in the ELR-treated samples. In contrast, the PEI polymer alone

F4

**TABLE I. Results of MALDI-TOF Analysis and Final Polymer Production Yield**

	Experimental MW (Da) (Mean ± SD)	Yield (mg/L)
IK120	51,996 ± 11.3	154
IMID-IK120	54,617 ± 7.9	65% <sup>a</sup>
IK120CPP	54,319 ± 4.3	35
LAELIK120CPP	55,696 ± 2.8	50

appeared to trigger marked aggregation processes at the same final concentration of 0.5 mg/mL.

With regard to the interaction between the polymers and the main protein components of plasma (IgM, fibrinogen, transferrin, and albumin), the electrophoresis patterns showed no interaction with the ELRs, whereas PEI induced the complete absence of fibrinogen and partial reduction in the other bands (Supporting Information Fig. S8). Accordingly, these results demonstrate that the ELRs studied herein are more compatible with blood components than PEI.

### Cell viability

The effect of the ELRs on cellular viability was tested in the adherent C6 glial tumoral cells. The findings [Fig. 5(A)] showed that the viability of cells incubated with ELRs was clearly higher than 100%, even at the highest concentration studied (450 µg/mL), and about 150% at a concentration of 100 µg/mL. The quantitative results were visually confirmed by way of the Live and Dead assay images, as shown in Fig. 5(B), where green (live) cells are predominant. Similar results were obtained with mesenchymal stem cells (data not shown). In contrast, highly cytotoxic effects of PEI were found [Fig. 5(A)]. The present ELRs, appear to be biocompatible toward both cultured adherent cells at high concentration and blood components.

F5

### DNA condensation ability and plasma-release assays

ELR-pDNA polyplexes were prepared at the specific (ELR)/(pDNA) weight ratios (from 10/1 to 140/1) and their complexation was evaluated in a gel-retardation experiment (Fig. 6). The strong interaction of these polymers with DNA reduces the mobility of the latter in the agarose gel. IK120CPP was the best polymer in terms of condensing

F6

**TABLE II. Transition Temperature ( $T_t$ ) and Enthalpy Change for the ELRs**

	$T_t$ (°C)	$\Delta H$ (Jg <sup>-1</sup> )
IK120	27.2	-6.8
IMID-IK120	22.1	-2.1
IK120CPP	31.3	-4.8
LAELIK120CPP	27.0	-4.1

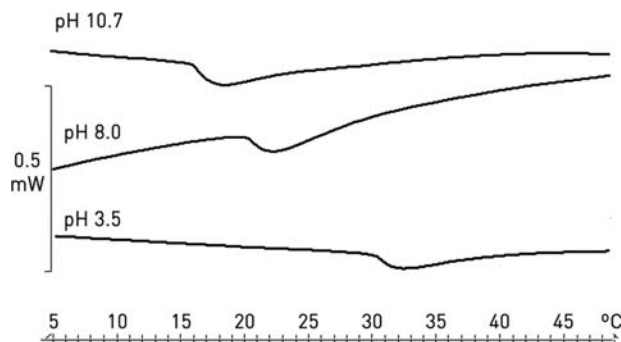


**FIGURE 2.** DSC for IMID-IK120 at different pH and at a concentration of 50 mg/mL in deionized water.

pDNA from 10/1 ratio. In contrast, LAELIK120CPP complexed pDNA better from 40/1 ratio and IMID-IK120 lost the pDNA at all the ratios tested.

Additionally, the stability of the nanocomplexes at different ratios when incubated with plasma was studied (Supporting Information Fig. S9). The data showed that the plasma altered the mobility of pDNA alone, retaining it in the well. Plasma components were able to compete with pDNA for polymer binding and displace it at a ratio of 10/1. The weak ability of IMID-IK120 polyplexes to condense pDNA was clarified, as shown by the fact that the strongest band appears at a 10/1 ratio. However, the ELR-pDNA interaction was sufficiently strong at ratios of 40/1 and higher; therefore ratios from 40/1 to 120/1 were chosen for physical characterization of the polyplexes.

**Determination of particle size and z-potential**

Size measurements showed the formation of ELR-pDNA polyplexes triggered by the presence of pDNA, which con-

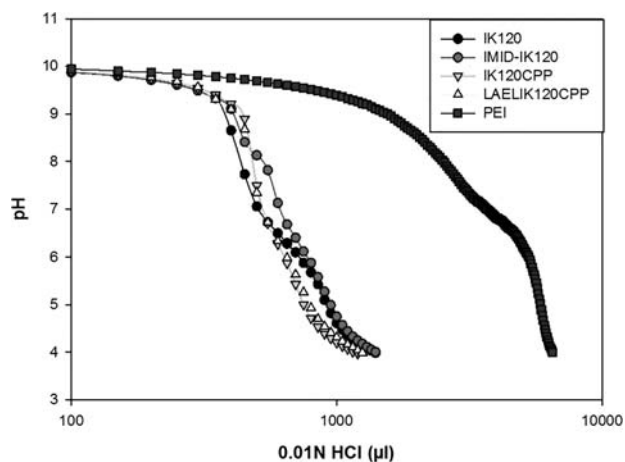


**FIGURE 3.** Buffering capacity of the ELRs compared with PEI 25 kDa in 0.9% NaCl solution. The x-axis is plotted in logarithmic scale to facilitate visualization of the data. [Color figure can be viewed in the online issue, which is available at wileyonlinelibrary.com.]

denses and promotes ELR complexation and self-assembly. The particle-size distribution for the resulting ELR-pDNA polyplexes varied from 150.0 to 309.4 nm (Table III). For IK120 and IMID-IK120, the particle size mainly decreased at high ratios. In contrast, the particle size for IK120CPP and LAELIK120CPP increased with amount of polymer (Table III). The formation of spherical nanoparticles was corroborated by TEM microscopy. All polyplexes showed a rounded shape and no major differences were observed between the ELRs (Fig. 7), with particle sizes being similar to those obtained with the DLS.

The resulting z-potential of the ELR-pDNA polyplexes ranged from +11.4 to +23.5 mV and are summarized in

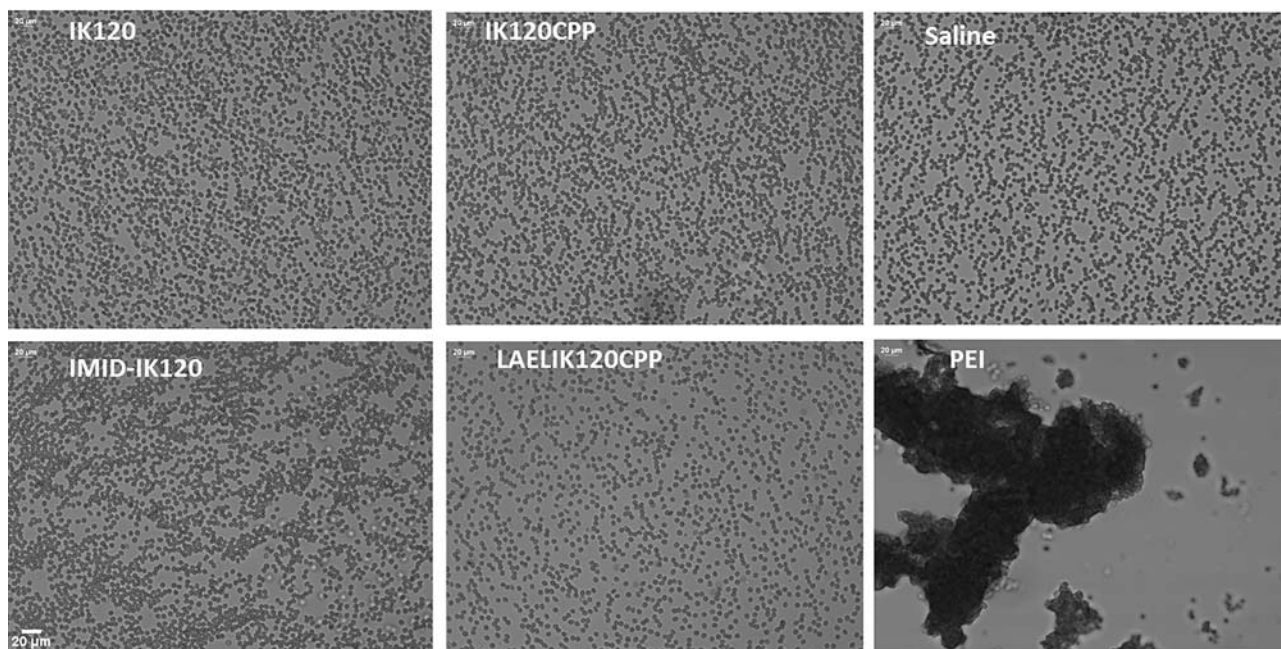


**FIGURE 4.** Aggregation studies of the red blood cell fraction with 0.5 mg/mL ELRs. Saline was used as negative control and 0.5 mg/mL PEI as control.

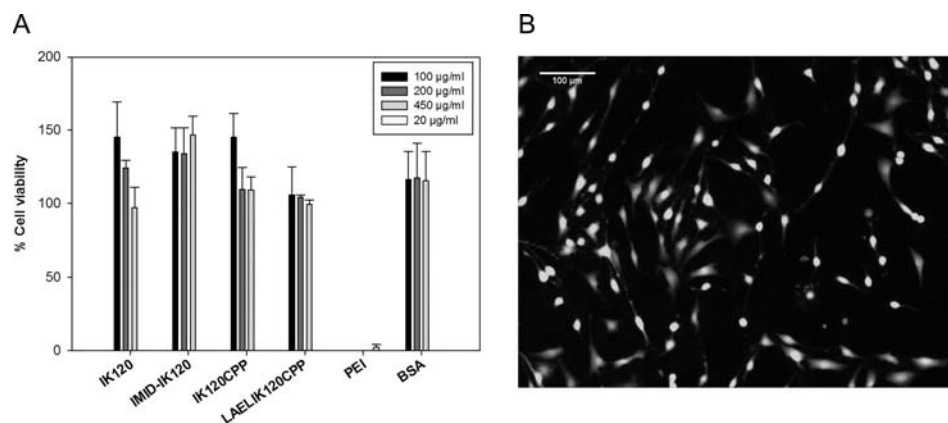


**FIGURE 5.** A. Cell viability of C6 cells incubated with ELRs at different concentrations, with PEI as reference polymer and BSA as negative and positive control, respectively. Cells were incubated with the polymer solutions for 24 h. Results are expressed as mean  $\pm$  standard error (SE). B. Live/Dead assay for C6 cells incubated with 200  $\mu\text{g}/\text{mL}$  IKCPP for 24 h. [Color figure can be viewed in the online issue, which is available at [wileyonlinelibrary.com](http://wileyonlinelibrary.com).]

T4 Table IV. The increase in z-potential value was found to be correlated with an increase in the amount of polymer at the 140/1 ratio. Specifically IMID-IK120 showed a lower zeta potential than IK120 at ratios of 40/1 and 80/1 due to substitution of the lysines, although both values were similar at higher ratios. The highest zeta potential was found for IK120CPP and LAELIK120CPP, both of which had a value of more than +20 mV due to the presence of arginine-enriched CPP, which provides more positive charge to the system.

**Cell transfection and trafficking assays**

In light of the previous assays, ELR-pDNA weight ratios of 80/1 and 120/1 showed the best physical features, namely a particle diameter around 200 nm and a zeta potential up to nearly +24 mV with high cell viability, for testing as ELR-based gene-delivery systems *in vitro*. Expression and localization of the genetic material transfected into the cells was determined by confocal fluorescence and quantified using the luciferase assay.

**p53 expression.** C6 glioma cells were selected as standard as this cell line is widely used for transfection, especially in glioblastoma research.<sup>33–35</sup> Plasmid DNA containing the p53 transgene was used to evaluate gene expression with ELRs as vectors over a prolonged time period (48 h). Successful delivery of the transgene into the nucleus was determined by the activation of apoptosis, as p53 gene expression is known to lead to cell death.<sup>37</sup> With this assay, significant death was observed for cells treated with all the different polyplexes formed with functionalized IK120 ELRs. However, the death effect was visibly higher in cells treated with polyplexes containing LAELIK120CPP at ratios of 80/1 and 120/1 in comparison with IK120 polyplexes and untreated control cells (Fig. 8). Nevertheless, there was no significant difference between the 80/1 and 120/1 ratios.

F8

**Polyplex cell internalization.** The localization of the polyplexes once transfected into C6 cells was evaluated using a confocal fluorescence microscope. The selected ratio for this test was 80/1 ratio as this gave together with 120/1 the

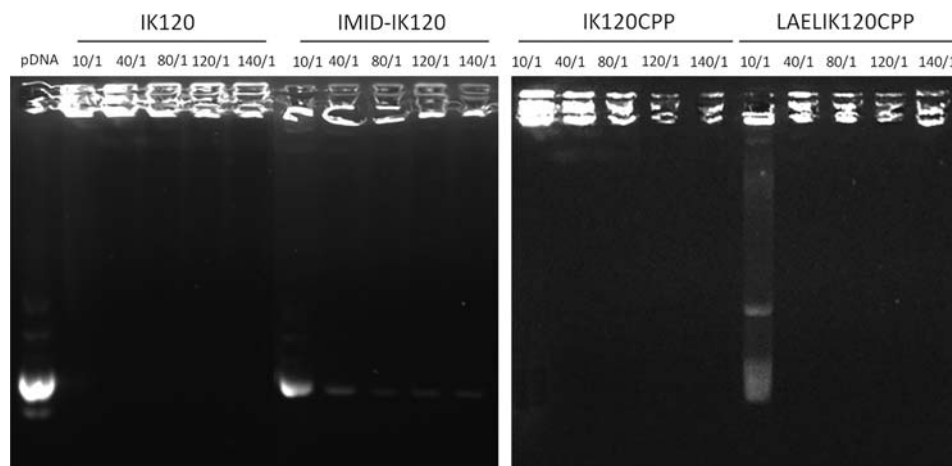


**FIGURE 6.** Agarose gel electrophoresis retardation assay at different ELR-pDNA (w/w) ratios. Polymer-free pDNA was used as control.

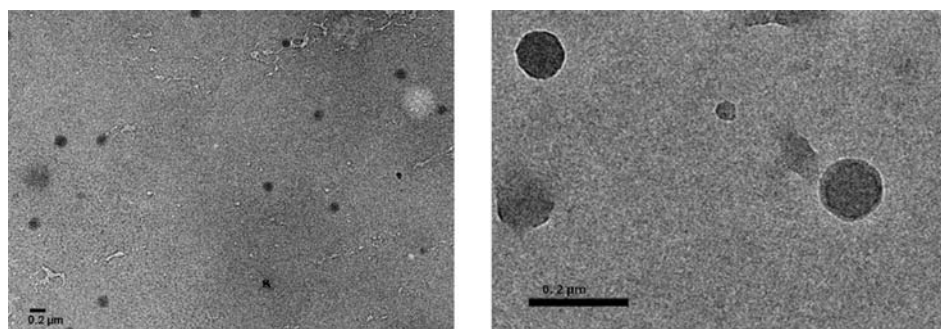


FIGURE 7. TEM images for polyplexes IK120CPP-pDNA (left side) and LAELIK120CPP-pDNA (right side). Both with a 0.2 μm bar scale.

F9 qualitative highest p53 expression for the IK120 modified polymers (Fig. 9). To this end, pDNA containing the p53 transgene was tagged with YOYO (green) and the nucleus stained with Hoechst (blue). A wide distribution of the plasmid in the cytoplasm and nucleus could be appreciated from the samples incubated with polyplexes (Fig. 9) at the selected weight ratio of 80/1. After 3 h of incubation with cells, the plasmid containing the p53 gene appeared in both the cytoplasm and the nucleus when complexed with IMID-IK120 and IK120CPP. In contrast, the plasmid carried by LAELIK120CPP was mainly located in the cytoplasm.

F10 **Luciferase transfection and expression.** The quantification of transfection by the polyplexes was accomplished using the luciferase assay. Luciferase expression in the cells treated with the ELR polyplexes showed significantly better results in comparison with the plasmid alone (Fig. 10). Specifically, polyplexes containing the LAELIK120CPP polymer exhibited more than fivefold higher luciferase expression than pDNA and more than twofold when comparing with the non-functionalized IK120. These results highlight the increasing improvement of transfection by incorporation of both penetratin and especially LAEL peptide into the lysine rich ELR construct.

**DISCUSSION**

Delivering efficiently genetic material into the cells by the use of nontoxic nonviral vectors is a bottleneck in the design of new gene delivery systems. For this purpose ELRs with biofunctional domains were developed by genetic engineering techniques allowing the full control over their composition and positioning them as an excellent alternative to other existing polymers. In the present study a lysine-based ELR was modified with several motifs in order to improve

the delivery of genetic material inside the cells with low cytotoxicity. As a result, two main strategies were adopted. The first strategy involved improving entry into the cell by designing an ELR with a bio-functional penetratin CPP domain derived from the Antennapedia transcription factor from *Drosophila melanogaster*. This is an amphiphilic peptide rich in arginines, with a positive charge at physiological pH, that is able to cross the cell membrane and enter the cytoplasm, thereby promoting the internalization of oligonucleotides, peptides and nanoparticles.<sup>38</sup> Penetratin was selected as the CPP of choice due to its high transfection efficiency and nontoxicity when complexed with ELRs.<sup>29</sup> When the polymeric vector enters the cell via the endocytic pathway, it is encapsulated in an endosome vesicle and therefore experiences a drop in pH from the physiological value to pH 6 in the endosome and pH 5 inside the lysosome.<sup>13</sup> The polymer and its DNA cargo would presumably be degraded by lysosomal enzymes. The second strategy involved stimulating endosome escape by two alternatives, namely recombinant incorporation of the fusogenic peptide “LAEL”<sup>39</sup> into the basic ELR sequence and chemical addition of imidazole functional groups with buffering capacity into the basic ELR polymer. As described in the literature, LAEL undergoes a structural change when the pH drops from physiological values to 5.0,<sup>39</sup> changing from a random coil to α-helix, thereby resulting in destabilization of the endosome membrane. In contrast, the modification with imidazole groups (pK<sub>a</sub> of 6.9) favors disruption of the endosome supported by the proton sponge hypothesis.<sup>10</sup> The protonation of imidazole at endosomal pH (pH 6) triggers an influx of water and ions, thereby destabilizing and disrupting the endosome. This strategy would improve the buffering capacity of the polymer and facilitate release of the polymer/pDNA complex into the cytoplasm.<sup>17,40</sup> The expected

**TABLE III. Particle Size (z-Average nm) for the ELR-pDNA Plasmid Nanocomplexes at Different Weight Ratios (Mean ± SD) in Deionized Water**

ELR/pDNA Ratio (w/w)	IK120	IMID-IK120	IK120CPP	LAELIK120CPP
40/1	292.1 ± 6.2	179.1 ± 4.1	171.9 ± 1.2	155.7 ± 2.2
80/1	272.7 ± 5.9	190.0 ± 4.0	175.1 ± 8.3	159.6 ± 1.7
120/1	173.0 ± 0.9	150.0 ± 1.8	246.5 ± 7.7	159.8 ± 2.1
140/1	229.2 ± 8.3	165.0 ± 9.6	309.4 ± 10.0	177.1 ± 3.9



**TABLE IV. Zeta Potential (mV) for the ELR-pDNA Plasmid Nanocomplexes at Different Weight Ratios (Mean  $\pm$  SD)**

ELP/pDNA Ratio (w/w)	IK120	IMID-IK120	IK120CPP	LAELIK120CPP
40/1	+13.6 $\pm$ 0.4	+11.4 $\pm$ 0.5	+19.1 $\pm$ 0.5	+15.6 $\pm$ 0.3
80/1	+13.7 $\pm$ 0.2	+12.6 $\pm$ 0.3	+21.2 $\pm$ 0.4	+18.1 $\pm$ 0.2
120/1	+13.9 $\pm$ 0.0	+13.8 $\pm$ 0.3	+23.4 $\pm$ 1.5	+21.4 $\pm$ 0.6
140/1	+14.2 $\pm$ 0.7	+14.1 $\pm$ 0.5	+23.5 $\pm$ 0.7	+21.5 $\pm$ 0.3

behavior of the imidazole groups by the aforementioned proton sponge mechanism was assessed by the variation in the IMID-IK120 polarity at the different pH as shown in Figure 2 and Supporting Information Table S1 and by the increase in the buffering capacity of the polymer at pH

range 8 to 6 in comparison with the others ELRs. Accordingly, modification of IK120 with imidazole functional groups at 65% substitution results in an increase in the proton-capturing tendency of the polymer.

The next step was to evaluate the biocompatibility of the ELRs. Although the ELR/pDNA nanocomplex has to be positively charged in order to interact with the cell membrane and ensure transfection, some aggregation processes with blood components may appear if this positive charge is too high, thus causing problems of cell lysis and clotting.<sup>41</sup> As such, the biocompatibility of ELRs with blood cells and plasma was addressed to ensure that the physiological fluid system of our body is able to tolerate the impact of the polymers, which is a prerequisite for gene-therapy applications. Blood cell aggregation studies (Fig. 4) showed no aggregation with any of the blood components in comparison with the striking aggregation process existing in the PEI treated samples. Additionally, the effect of the ELRs on cellular viability was tested in the adherent C6 glial tumoral cells. Our findings [Fig. 5(A)] showed that the viability of cells incubated with ELRs was clearly higher than 100%, even at the highest concentration studied (450  $\mu$ g/mL), and about 150% at a concentration of 100  $\mu$ g/mL. Similar viability levels over 100% had been previously obtained on mouse myoblastoma cell line,<sup>42,43</sup> in human breast cancer cell line<sup>44</sup> and mesenchymal stem cell<sup>42,45</sup> when cells were incubated with ELRs nano/microparticles, thereby demonstrating the innocuous behavior of these polymers.<sup>46</sup> The quantitative results were visually confirmed by way of the Live and Dead assay images, as shown in Figure 5(B), where green (live) cells are predominant. Similar results were obtained with mesenchymal stem cells (data not shown). In contrast, highly cytotoxic effects of PEI were found [Fig. 5(A)], which had been previously reported for the C6 glioma cell line<sup>47</sup> and in 293T from human kidney above 4  $\mu$ g/mL.<sup>48,49</sup> PEI produces nonspecific cytotoxicity as a result of destabilization of the plasmatic and mitochondrial membranes, which triggers the activation of apoptotic pathways, thereby restricting its clinical application.<sup>50–52</sup> The present ELRs, however, appear to be biocompatible toward both cultured adherent cells at high concentration and blood components, both of which are aspects that must be considered when developing gene-therapy strategies.

ELR-pDNA polyplexes were prepared at specific (ELR)/(pDNA) weight ratios. The condensation of DNA-forming nanocomplexes is a critical step that influences their entry into cells but also their stability and protection against nucleases attack.<sup>53</sup> In this case, the electrostatic interactions between the amino groups from the polymer and the

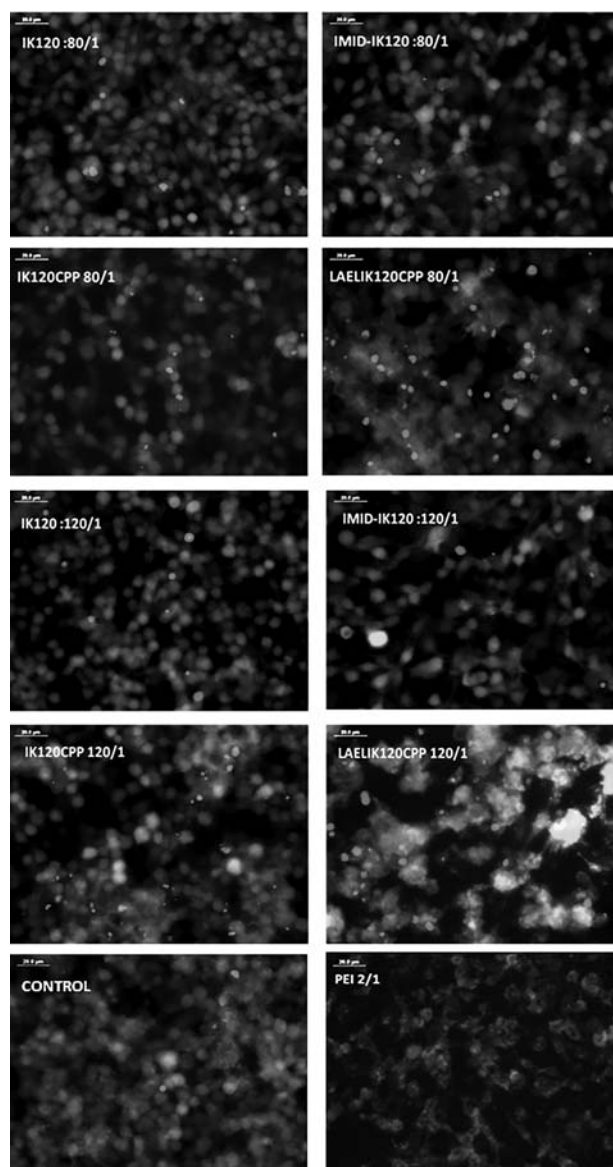


**FIGURE 8.** Live/Dead assay for C6 cells transfected with ELR-p53 plasmid and PEI-p53 plasmid polyplexes at different weight ratios. Live cells are stained green and dead cells red. Cells visualized using an inverted fluorescence microscope. [Color figure can be viewed in the online issue, which is available at [wileyonlinelibrary.com](http://wileyonlinelibrary.com).]

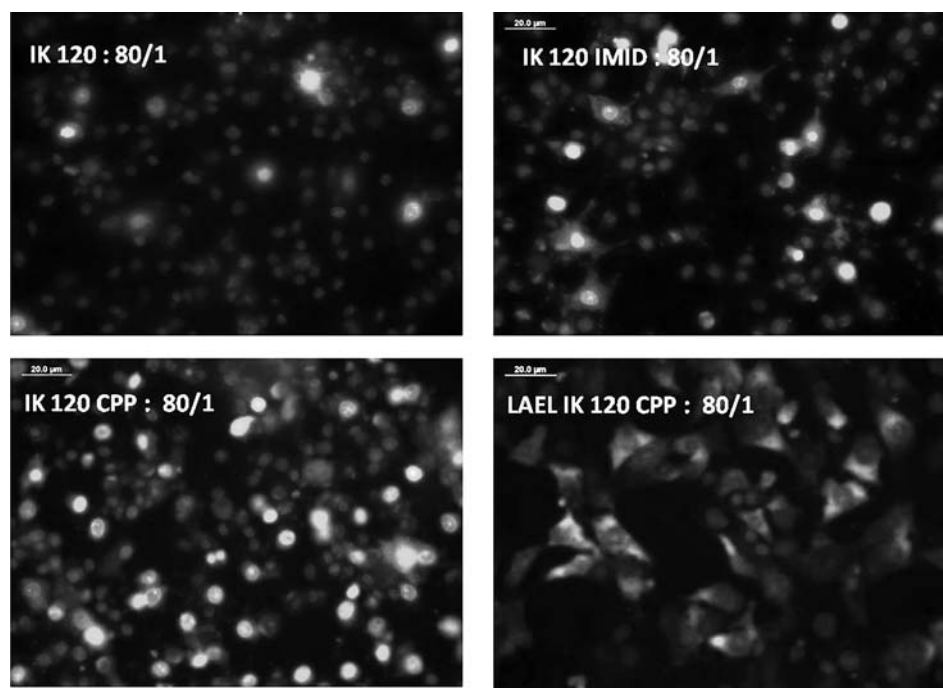


**FIGURE 9.** Cellular localization of pDNA in C6 cells. ELR polyplexes were formed with pDNA tagged with YOYO and ELR at (w/w) ratio of 80/1 and incubated with C6 cells for 3 h. YOYO-tagged DNA appears green and the nucleus is blue as a result of Hoechst stain. Cells visualized by inverted fluorescence microscopy. [Color figure can be viewed in the online issue, which is available at [wileyonlinelibrary.com](http://wileyonlinelibrary.com).]

negatively charged phosphate groups from the backbone of the DNA allow this complexation, which was evaluated in a gel-retardation experiment (Fig. 6). IK120CPP had the highest and IMID-IK120 polymer the lowest condensation ability with the pDNA. The explanation for this finding for IMID-IK120 lies in the fact that this polymer only contains 10 free lysines, with the remaining 15 being substituted by imidazole groups, thus meaning that IMID-IK120 was less able to condense pDNA than the non-modified polymer. In addition, an appropriate stability of the resulting polyplex is

required in order to protect the genetic material during trafficking through the physiological environment. Charged serum components, such as albumin, may destabilize the polyplex by competitive binding or by cationic polymer displacement.<sup>36</sup> As shown in the Supporting Information Figure S9, the obtained polyplexes were sufficiently stable especially for IK120CPP and LAELIK120CPP.

The resulting polyplexes showed a particle size from 150.0 to 309.4 nm (Table III). This range is appropriate for cellular uptake, and particles of this size are thought to be internalized mainly via clathrin-dependent or -independent endocytosis phenomena.<sup>13,54</sup> The size of polyplexes made of synthetic polycations may be sensitive to kinetic factors as concentration, temperature, or mixing speed.<sup>55,56</sup> In our study we showed that the presence of a sufficiently content of ELR was necessary for the good stability of the polyplexes (Fig. 6 and Supporting Information Fig. S9). For this reason we hypothesized that from (ELR)/(pDNA) weight ratio of 40/1 the polyplexes were stable and the temperature change from mixing (10 °C) to the application *in vitro* (37 °C) would not affect significantly to their particle size. Additionally, the mixing method used in this study guaranteed the homogeneous distribution of the ELR concentration in the sample and showed the presence of homogeneous particle size populations (Supporting Information Fig. S10). In contrast the particle size was influenced by the concentration of ELR. For IK120 and IMID-IK120, the particle size mainly decreased at high ratios due to the ability of these polymers to pack tightly. However, the particle size for IK120CPP and LAELIK120CPP increased with amount of polymer due to the progressive increase in repulsive forces

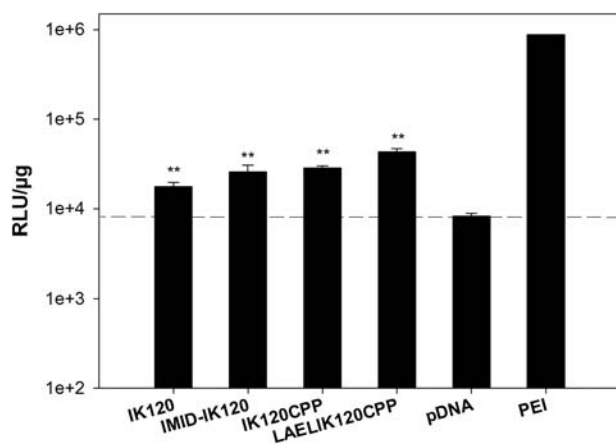


**FIGURE 10.** Luciferase expression for different polyplex treatments. C6 cells were transfected with ELR/pDNA polyplexes at an 80/1 weight ratio. Luciferase activity was evaluated 48 h post-transfection and expressed in RLU/μg protein lysate. pDNA was used as negative control. The results are expressed in logarithmic scale as mean ± standard error of three independent experiments. \*\**p* < 0.05.

inside the polyplex favored by the presence of the hydrophilic CPP. The stability of many colloidal systems is directed related to the magnitude of their zeta potential. Thus, if the value of the z-potential from the particle is high (around +30 mV), the colloidal system will usually be stable. In contrast, if this value is around 0 mV the system will tend to agglomerate. The resulting z-potential of the ELR-pDNA polyplexes was up to +23.5 mV (Table IV). The positive z-potential suggests the distribution of positive charges from the polymer on the periphery of the polyplexes. A positive z-potential is thought to improve cellular internalization as a result of interaction with the negatively charged plasmatic membrane.<sup>12</sup>

After these analysis, ELR-pDNA weight ratios of 80/1 and 120/1 showed the best physical characteristics for transfection in *in vitro* assays. Initially the expression and localization of plasmid DNA containing the p53 gene was evaluated by confocal fluorescence and quantified by the luciferase system.

The expression of p53 gene was evaluated by a Live and Dead assay where cells were incubated with the ELR-pDNA polyplexes (Fig. 8). The maximum polymer concentration reached was 300 µg/mL, which corresponds to the highest ratio (120/1). At this concentration, according to the cytotoxicity assays, the cell viability for ELRs was 100%, thereby suggesting that cell death is mainly due to the effect of the p53 gene transfected into C6 glioma cells. The results showed the higher cellular death in cells treated with LAELIK120CPP polyplexes in contrast to the IMID-IK120. Thereby, suggesting that the role of the LAEL fusogenic peptide is essential to endosome escape by the polyplex rather than the sponge effect mediated by the imidazole groups. Interestingly, when incubated at a weight ratio of 2/1, PEI induced a high level of cell death. One likely explanation for this effect given the previously reported cytotoxic effects of PEI is that cell death, after transfection with PEI at these conditions, was probably due further by the p53 transgene expression but also in lesser extent by the polymer itself.

Fluorescence microscopy was also used to localize the polyplexes once transfected into C6 cells (Fig. 9). The natural ability of penetratin to cross the plasmatic membrane and facilitate the intracellular delivery of macromolecules by either direct translocation or the endosomal or macropinocytosis pathways is well known.<sup>57-59</sup> In this assay, penetratin favored the presence of the plasmid in the cytoplasm and even inside the nucleus in cells transfected with the IKCPP-pDNA polyplexes. However, in the case of polyplexes containing LAELIK120CPP, penetratin also triggered their internalization but the LAEL peptide seemed to facilitate the destabilization of the endosome membrane and the escape of the pDNA into the cytoplasm, where it was extensively located after the first 3 h of incubation. Similarly, the imidazole groups in IMID-IK120 promoted the leakage of pDNA from the endosome. Histidinylated oligo(ethanamino)amides have recently been found to have enhanced transfection properties mediated by their increased buffering capacity at endosomal pH.<sup>60</sup> The known "proton sponge effect"<sup>10</sup> appeared to boost some cytoplasmic and even nuclear presence of the

plasmid. The widespread location of the polyplexes containing LAELIK120CPP at a ratio of 80/1 in the first 3 h, and the high expression of p53 gene after 48 h, suggest a slower but more efficient endosomal mechanism of escape governed by the LAEL peptide than for imidazole groups.

Finally, the quantification of transfection by the polyplexes was necessary for the direct application of these ELRs in gene therapy (Fig. 10). The incorporation of functional internalization peptides to lysine enriched ELR were necessary for higher transfection efficiency levels. Indeed, polyplexes containing the LAELIK120CPP polymer exhibited the highest luciferase expression with more than fivefold than pDNA. Once the polyplexes are inside the endosome, LAEL seems to play a key role in leakage of the pDNA from the endosome. After incubation for 5 h, the luciferase pDNA delivered by LAELIK120CPP was able to reach the nucleus. In contrast, the main role of penetratin appears to be during cell entry and it is not as important as regards endosomal escape even though some plasmid still reaches the nucleus. Additionally, LAEL seems to promote slower but more efficient outflow of the imidazole groups bound to the lysine-rich polymer. Hence, LAEL plays a more relevant role in transfection than CPP alone and incorporation of imidazole groups. Lower transfection efficiency for ELRs was found when comparing with PEI due to their lower charge density that may give to the ELRs more compatible features. Similar results of transfection had been previously reported for ELRs appended with oligo-lysine or p [Asp(DET)]53 in comparison with BPEI,<sup>61,62</sup> where despite of its toxicity, PEI was also selected to compare luciferase expression levels due to its good transfection properties.<sup>63,64</sup> Taking together, the previous research of ELR as nonviral vectors showed higher toxicity than the ELRs developed in this work, with a viability up to 70% for the oligo-lysine modified ELR and from 80% for p [Asp(DET)]53. The first was formed by an ELR-based diblock bearing an oligo-lysine for pDNA condensation. The second was constituted by an ELR-based diblock containing diethylenetriamine (DET) modified poly-L-aspartic acid segment which conferred less toxicity. Herein we report cationic and highly biocompatible ELRs with acquired functionalities able to condense and transfer genetic material by themselves which represents a breakthrough in this regard. In light to the results in biocompatibility, extensively future experiments are warranted focusing in increasing the charge density of the polyplexes in order to get similar results than others polymers such as PEI together with *in vivo* evaluation of the transfection.

## CONCLUSION

We have designed, constructed, produced, and tested novel and highly biocompatible ELR materials with different functionalities for gene-delivery applications. Unlike other polymeric systems such as PEI or virus-derived vectors, these ELRs possess a marked potential for protein modifications by recombinant techniques in a totally controlled manner. Notably, the analyzed ELRs exhibited high levels of viability *in vitro* which is a striking contrast to PEI cytotoxicity.

Indeed, incorporation of acquired functionalities provided by the CPP, LAEL peptides, or protonable imidazole groups provided higher levels of internalization and gene expression in comparison with the polyplexes formed either by the nonmodified ELR or pDNA. All the ELR-pDNA polyplexes studied showed cellular entry, with this being higher in the case of LAELIK120CPP complexes. Penetratin plays a role in the first step of the internalization process, namely cellular entry of the polyplexes, whereas LAEL and imidazole groups to a lesser extent governed endosomal escape of the pDNA via their fusogenic activity and proton sponge effect, respectively. Future studies will be focused on improving the transfection efficiency of these systems, due to their high cytocompatibility and versatility, thus endowing them with great potential in gene-therapy applications.

## REFERENCES


- Ginn SL, Alexander IE, Edelstein ML, Abedi MR, Wixon J. Gene therapy clinical trials worldwide to 2012 – An update. *J Gene Med* 2013;15:65–77.
- Manfredsson FP, Bloom DC, Mandel RJ. Regulated protein expression for in vivo gene therapy for neurological disorders: Progress, strategies, and issues. *Neurobiol Dis* 2012;48:212–221.
- Alex SM, Rekha MR, Sharma CP. Spermine grafted galactosylated chitosan for improved nanoparticle mediated gene delivery. *Int J Pharm* 2011;410:125–137.
- Yla-Herttuala S. Cardiovascular gene therapy with vascular endothelial growth factors. *Gene* 2013;525:217–219.
- Niven R, Pearlman R, Wedeking T. Biodistribution of radiolabeled lipid-DNA complexes and  $^{64}\text{Cu}$  in mice. *J Pharm Sci* 1998; 87:1292–1299.
- Yin H, Kanasty RL, Eltoukhy AA, Vegas AJ, Dorkin JR, Anderson DG. Nonviral vectors for gene-based therapy. *Nat Rev Genet* 2014;15:541–555.
- Hosel M, Broxtermann M, Janicki H. Toll-like receptor 2-mediated innate immune response in human nonparenchymal liver cells toward adeno-associated viral vectors. *Hepatology* 2012;55:287–297.
- Mays LE, Vandenbergh LH, Xiao R. Adeno-associated virus capsid structure drives CD4-dependent  $\text{CD}8^+$  T cell response to vector encoded proteins. *J Immunol* 2009;182:6051–6060.
- Anderson WF. Human gene therapy. *Nature* 1998;392(6679 Suppl):25–30.
- Midoux P, Pichon C, Yaouanc JJ, Jaffres PA. Chemical vectors for gene delivery: A current review on polymers, peptides and lipids containing histidine or imidazole as nucleic acids carriers. *Br J Pharmacol* 2009;157:166–178.
- Mintzer MA, Simanek EE. Nonviral vectors for gene delivery. *Chem Rev* 2009;109:259–302.
- Blau S, Jubeh TT, Haupt SM, Rubinstein A. Drug targeting by surface cationization. *Crit Rev Ther Drug Carrier Syst* 2000;17:425–465.
- Sahay G, Alakhova DY, Kabanov AV. Endocytosis of nanomedicines. *J Control Release* 2010;145:182–195.
- Kosuge M, Takeuchi T, Nakase I, Jones AT, Futaki S. Cellular internalization and distribution of arginine-rich peptides as a function of extracellular peptide concentration, serum, and plasma membrane associated proteoglycans. *Bioconjug Chem* 2008;19: 656–664.
- Thoren PE, Persson D, Isakson P, Goksor M, Onfelt A, Norden B. Uptake of analogs of penetratin, tat(48-60) and oligoarginine in live cells. *Biochem Biophys Res Commun* 2003;307:100–107.
- Lee H, Jeong JH, Park TG. PEG grafted polylysine with fusogenic peptide for gene delivery: High transfection efficiency with low cytotoxicity. *J Control Release* 2002;79:283–291.
- Thomas JJ, Rekha MR, Sharma CP. Unraveling the intracellular efficacy of dextran-histidine polycation as an efficient nonviral gene delivery system. *Mol Pharm* 2012;9:121–134.
- Rekha MR, Sharma CP. Hemocompatible pullulan-polyethyleneimine conjugates for liver cell gene delivery: In vitro evaluation of cellular uptake, intracellular trafficking and transfection efficiency. *Acta Biomater* 2011;7:370–379.
- Hunter AC. Molecular hurdles in polyfectin design and mechanistic background to polycation induced cytotoxicity. *Adv Drug Deliv Rev* 2006;58:1523–1531.
- Grigsby CL, Leong KW. Balancing protection and release of DNA: Tools to address a bottleneck of nonviral gene delivery. *J R Soc Interface* 2010;7(Suppl 1):S67–S82.
- Al-Dosari MS, Gao X. Nonviral gene delivery: Principle, limitations, and recent progress. *AAPS J* 2009;11:671–681.
- Rodriguez-Cabello JC, Martin L, Girotti A, Garcia-Arevalo C, Arias FJ, Alonso M. Emerging applications of multifunctional elastin-like recombinamers. *Nanomedicine* 2011;6:111–122.
- Pierna M, Santos M, Arias FJ, Alonso M, Rodriguez-Cabello JC. Efficient cell and cell-sheet harvesting based on smart surfaces coated with a multifunctional and self-organizing elastin-like recombinamer. *Biomacromolecules* 2013;14:1893–1903.
- Shi P, Gustafson JA, MacKay JA. Genetically engineered nanocarriers for drug delivery. *Int J Nanomed* 2014;9:1617–1626.
- Urry DW. What Sustains Life? Consilient Mechanisms for Protein-Based Machines and Materials. New York: Springer-Verlag; 2006.
- Sallach RE, Cui W, Balderrama F. Long-term biostability of self-assembling protein polymers in the absence of covalent crosslinking. *Biomaterials* 2010;31:779–791.
- Arias FJ, Santos M, Fernandez-Colino A, Pinedo G, Girotti A. Recent contributions of elastin-like recombinamers to biomedicine and nanotechnology. *Curr Top Med Chem* 2014;14:819–836.
- Walker L, Perkins E, Kratz F, Raucher D. Cell penetrating peptides fused to a thermally targeted biopolymer drug carrier improve the delivery and antitumor efficacy of an acid-sensitive doxorubicin derivative. *Int. J. Pharm.* 2012;436:825–832.
- Bidwell GL, Raucher D. Cell penetrating elastin-like polypeptides for therapeutic peptide delivery. *Adv Drug Deliv Rev* 2010;62: 1486–1496.
- Rodriguez-Cabello JC, Girotti A, Ribeiro A, Arias FJ. Synthesis of genetically engineered protein polymers (recombinamers) as an example of advanced self-assembled smart materials. *Methods Mol Biol* 2012;811:17–38.
- Girotti A, Reguera J, Arias FJ, Alonso M, Testera AM, Rodriguez-Cabello JC. Influence of the molecular weight on the inverse temperature transition of a model genetically engineered Elastin-like pH-responsive polymer. *Macromolecules* 2004;37:3396–3400.
- Sallach RE, Cui W, Balderrama F. Long-term biostability of self-assembling protein polymers in the absence of covalent crosslinking. *Biomaterials* 2010;31:779–791.
- Angelastro JM, Lame MW. Overexpression of cd133 promotes drug resistance in c6 glioma cells. *Mol Cancer Res* 2010;8:1105–1115.
- Naus CC, Elisevich K, Zhu D, Belliveau DJ, Del Maestro RF. In vivo growth of c6 glioma cells transfected with connexin43 cDNA. *Cancer Res* 1992;52:4208–4213.
- Li G, Li W, Angelastro JM, Greene LA, Liu DX. Identification of a novel DNA binding site and a transcriptional target for activating transcription factor 5 in c6 glioma and mcf-7 breast cancer cells. *Mol Cancer Res* 2009;7:933–943.
- Srinivasachari S, Liu Y, Prevette LE, Reineke TM. Effects of trehalose click polymer length on pDNA complex stability and delivery efficacy. *Biomaterials* 2007;28:2885–2898.
- Haupt S, Berger M, Goldberg Z, Haupt Y. Apoptosis - The p53 network. *J Cell Sci* 2003;116:4077–4085.
- Bechara C, Sagan S. Cell-penetrating peptides: 20 years later, where do we stand? *FEBS Lett* 2013;587:1693–1702.
- Ohmori N, Niidome T, Wada A, Hirayama T, Hatakeyama T, Aoyagi H. The enhancing effect of anionic alpha-helical peptide on cationic peptide-mediated transfection systems. *Biochem Biophys Res Commun* 1997;235:726–729.
- Akinc A, Thomas M, Klibanov AM, Langer R. Exploring polyethyleneimine-mediated DNA transfection and the proton sponge hypothesis. *J Gene Med* 2005;7:657–663.
- Jokerst JV, Lobovkina T, Zare RN, Gambhir SS. Nanoparticle PEGylation for imaging and therapy. *Nanomedicine (Lond)* 2011; 6:715–728.
- Costa RR, Girotti A, Santos M, Arias FJ, Mano JF, Rodriguez-Cabello JC. Cellular uptake of multilayered capsules produced

AQ2


- with natural and genetically engineered biomimetic macromolecules. *Acta Biomater* 2014;10:2653–2662.
43. Bessa PC, Machado R, Nurnberger S, et al. Thermoresponsive self-assembled elastin-based nanoparticles for delivery of BMPs. *J Control Release* 2010;142:312–318.
  44. Sarangthem V, Cho EA, Bae SM, et al. Construction and application of elastin like polypeptide containing IL-4 receptor targeting peptide. *PLoS ONE* 2013;8:e81891
  45. Dash BC, Mahor S, Carroll O, et al. Tunable elastin-like polypeptide hollow sphere as a high payload and controlled delivery gene depot. *J Control Release* 2011;152:382–392.
  46. Garcia-Arevalo C, Pierna M, Girotti A, Arias FJ, Rodriguez-Cabello JC. A comparative study of cell behavior on different energetic and bioactive polymeric surfaces made from elastin-like recombinamers. *Soft Matter* 2012;8:3239–3249.
  47. Alex SM, Sharma CP. Enhanced intracellular uptake and endocytic pathway selection mediated by hemocompatible ornithine grafted chitosan polycation for gene delivery. *Colloids Surf B Biointerfaces* 2014;122:792–800.
  48. Deng R, Yue Y, Jin F, et al. Revisit the complexation of PEI and DNA - How to make it nontoxic and highly efficient PEI gene transfection nonviral vectors with a controllable chain length and structure? *J Control Release* 2009;140:40–46.
  49. Choi YJ, Kang SJ, Kim YJ, Lim YB, Chung HW. Comparative studies on the genotoxicity and cytotoxicity of polymeric gene carriers polyethylenimine (PEI) and polyamidoamine (PAMAM) dendrimer in jurkat T-cells. *Drug Chem Toxicol* 2010;33:357–366.
  50. Hunter AC. Molecular hurdles in polyfectin design and mechanistic background to polycation induced cytotoxicity. *Adv Drug Deliv Rev* 2006;58:1523–1531.
  51. Fischer D, Li Y, Ahlemeyer B, Krieglstein J, Kissel T. In vitro cytotoxicity testing of polycations: Influence of polymer structure on cell viability and hemolysis. *Biomaterials* 2003;24:1121–1131.
  52. Moghimi SM, Symonds P, Murray JC, Hunter AC, Debska G, Szewczyk A. A two-stage poly(ethylenimine)-mediated cytotoxicity: Implications for gene transfer/therapy. *Mol Ther* 2005;11:990–995.
  53. O'Rourke S, Keeney M, Pandit A. Nonviral polyplexes: Scaffold mediated delivery for gene therapy. *Prog Polym Sci* 2010;35:441–458.
  54. Le Roy C, Wrana JL. Clathrin- and non-clathrin-mediated endocytic regulation of cell signalling. *Nat Rev Mol Cell Biol* 2005;6:112–126.
  55. Oupicky D, Konak C, Ulbrich K, Wolfert MA, Seymour LW. DNA delivery systems based on complexes of DNA with synthetic polycations and their copolymers. *J Control Release* 2000;65:149–171.
  56. Zelphati O, Nguyen C, Ferrari M, Felgner J, Tsai Y, Felgner PL. Stable and monodisperse lipoplex formulations for gene delivery. *Gene Ther* 1998;5:1272–1282.
  57. Heitz F, Morris MC, Divita G. Twenty years of cell-penetrating peptides: From molecular mechanisms to therapeutics. *Br J Pharmacol* 2009;157:195–206.
  58. Gupta B, Levchenko TS, Torchilin VP. Intracellular delivery of large molecules and small particles by cell-penetrating proteins and peptides. *Adv Drug Deliv Rev* 2005;57:637–651.
  59. Tahara K, Yamamoto H, Kawashima Y. Cellular uptake mechanisms and intracellular distributions of polysorbate 80-modified poly (D,L-lactide-co-glycolide) nanospheres for gene delivery. *Eur J Pharm Biopharm* 2010;75:218–224.
  60. Lachelt U, Kos P, Mickler FM, et al. Fine-tuning of proton sponges by precise diaminoethanes and histidines in pDNA polyplexes. *Nanomedicine* 2014;10:35–44.
  61. Chen T-H, Bae Y, Furgeson D. Intelligent biosynthetic nanobiomaterials (IBNs) for hyperthermic gene delivery. *Pharm Res* 2008;25:683–691.
  62. Chen TH, Bae Y, Furgeson DY, Kwon GS. Biodegradable hybrid recombinant block copolymers for nonviral gene transfection. *Int J Pharm* 2012;427:105–112.
  63. Höbel S, Aigner A. Polyethylenimines for siRNA and miRNA delivery in vivo. *Wiley Interdiscip Rev Nanomed Nanobiotechnol* 2013;5:484–501.
  64. Wiseman JW, Goddard CA, McLelland D, Colledge WH. A comparison of linear and branched polyethylenimine (PEI) with DCChol/DOPE liposomes for gene delivery to epithelial cells in vitro and in vivo. *Gene Ther* 2003;10:1654–1662.

Author Proof

AQ1: Kindly check whether the short title is OK as given 

AQ2: Kindly replace “et al.” with the missing autor names in all “et al.-type” reference 

AQ3: Please confirm that given names (red) and surnames/family names (green) have been identified correctl 

AQ4: Please confirm whether the color figures should be reproduced in color or black and white in the print version. If the color figures must be reproduced in color in the print version, please fill the color charge form immediately and return to Production Editor. Or else, the color figures for your article will appear in color in the online version only 

WILEY  
Author Proof